Hindawi
Advances in Materials Science and Engineering
Volume 2022, Article ID 7778328, 11 pages
https://doi.org/10.1155/2022/7778328

Research Article

Structural, Morphological, Optical, and Antibacterial Activities of Zinc Oxide Nanopowders: A Comparative Study of Green and Soft Chemical Synthesis

K. Catherine Siriya Pushpa,[1] **P. Sakthivel**,[2] **K. Saravanakumar**,[3] **N. Anuradha**,[1] **R. K. Sankaranarayanan**,[4] **and Mosae Selvakumar Paulraj**[5]

[1]*Post-Graduate and Research Department of Physics, Bon Secours College for Women, Thanjavur 613006, Tamil Nadu, India*
[2]*Centre for Materials Science, Department of Physics, Science and Humanities, Faculty of Engineering, Karpagam Academy of Higher Education, Coimbatore 641021, India*
[3]*Department of Physics, Mahendra Institute of Technology (Autonomous), Mallasamudram, Namakkal 637503, Tamil Nadu, India*
[4]*Centre for Nano Science and Technology, Department of Chemistry, Chennai Institute of Technology, Kundrathur 600069, Tamil Nadu, India*
[5]*AUW Chemistry Hub, Science and Math Program, Asian University for Women, Chattogram, Bangladesh*

Correspondence should be addressed to P. Sakthivel; sakthi1807@gmail.com and Mosae Selvakumar Paulraj; p.selvakumar@auw.edu.bd

Received 14 May 2022; Revised 27 July 2022; Accepted 18 August 2022; Published 6 September 2022

Academic Editor: Zhongchang Wang

Copyright © 2022 K. Catherine Siriya Pushpa et al. This is an open access article distributed under the Creative Commons Attribution License, which permits unrestricted use, distribution, and reproduction in any medium, provided the original work is properly cited.

Zinc oxide, a well-known inorganic metal oxide in nanoparticle form, has outstanding antibacterial properties. In this work, the authors focus on determining ZnO nanoparticles' structural, optical, and antibacterial activity. A simple soft chemical route synthesizes C-ZnO nanoparticles chemically, while the green synthesis method is used to prepare G-ZnO nanoparticles. Ocimum tenuiflorum leaf extract was used to prepare G-ZnO nanopowders. These samples are investigated and compared in terms of their structural, morphological, optical, and antibacterial properties. According to XRD investigations, the synthesized ZnO nanopowders possess a hexagonal structure. The particle size of G-ZnO is smaller than that of C-ZnO nanoparticles. The XPS result revealed the binding and interactions between molecules. The FTIR study confirmed the presence of molecules and their vibrations. UV-vis-DRS spectroscopy was used to investigate optical properties such as reflectance and band gap. The grain size of the G-ZnO nanopowders was decreased, and oxygen vacancy was produced. The antibacterial efficiency of plant extracts against two different bacterial strains, *S. aureus* (Gram-positive) and E.*coli* (Gram-negative), has been studied and reported.

1. Introduction

The unique properties of zinc oxide nanoparticles like electrical, optical, gas-sensing, dermatological, and antibacterial are being utilized for diverse applications [1–3]. Such attractive properties make them promising candidates in widely distributed fields like medicine, electronics, drug delivery, optoelectronics, automobiles, textiles, and cosmetics. It has also been demonstrated that zinc oxide removes some dyes and water pollutants from textile effluent when exposed to UV light [4–8].

ZnO is one of the prime and active materials that exhibit excellent antibacterial activity. The usage of a capping agent can control the surface morphology. The release of antimicrobial ions, reactive oxygen species generation, and electrostatic interaction are important antibacterial mechanisms [9]. Antibacterial activity was proven to be size-dependent by the studies [10]. In earlier research, enhanced

bacteria-killing capacity was discussed in ZnO nanoparticles [11]. Many researchers have examined and reported the antibacterial activity of ZnO [12, 13].

There are many techniques reported for synthesizing ZnO nanoparticles (chemical synthesis methods: sol-gel process, combustion, sonochemical, coprecipitation, microwave-assisted, hydrothermal, and other soft chemical methods) [14–16]. These chemical processes result in the adsorption of some harmful chemical species on the surface, which may have negative consequences in specific applications. The utilized chemicals are harmful, resulting in non-eco-friendly products [17, 18].

The optimum zinc oxide nanomaterial concentration was discussed for different biological applications [19, 20]. The synthesis method plays an essential role in addressing the properties of materials and appending them for diverse applications. The difference between chemical and biological methods was discussed and reported [19, 21].

The high cost and use of toxic chemicals, as well as the harsh conditions for reduction and stabilization, may be driving interest in the green synthesis methodology. Biological entities such as microorganisms and plant biomass are used for the eco-friendly assembly of nanoparticles. The green synthesized ZnO nanoparticles have some advantages over the chemically synthesized ZnO nanoparticles. Various researchers have discussed the importance of green synthesis [22–24].

Nowadays, the attention of researchers is growing toward the biosynthesis of metal nanoparticles using organisms. Of these organisms, plants play a major role, and they seem to be the best candidates for the biosynthesis of nanoparticles. This attraction towards biosynthesis using plants is because nanoparticles are more stable and more varied in shape and size than those produced by chemical methods. Furthermore, the utilization of plant extracts reduces the cost of microbe isolation and culture media, and at the same time, it improves the cost-effectiveness of microbe nanoparticle synthesis. Because of its simplicity, eco-friendliness, and vast antibacterial efficacy, the biological approach to synthesizing zinc oxide (ZnO) nanoparticles has attracted much interest [25, 26]. Some plant components, such as roots, leaves, stems, seeds, and fruits, have also been used for zinc oxide nanoparticle synthesis, as plant extracts are rich in phytochemicals, which act as reducing and stabilizing agents.

Some of the plant leaf extracts are used to synthesize zinc oxide nanoparticles such as *Azadirachta indica*, *Agathosma betulina*, *Aloe vera*, *Parthenium hysterophorus L.*, *Plectranthus amboinicus*, *Vitex negundo L.*, *Costus pictus D. Don,* and *Pongamia pinnata*.

The green synthesized ZnO nanostructures showed antibacterial efficacy against Gram-positive and Gram-negative pathogens. Furthermore, synergistic effects of ZnO nanostructures and streptomycin showed increased effectiveness [27]. Biocompatibility has been explored via biosynthesized metal applications and biomedical and antimicrobial activities. The influence of plant extracts on the structural, surface morphological, optical, and particle nucleation processes is well described in earlier research [28–30]. Ocimum tenuiflorum is commonly present in tropical regions. The chemical constituents of Ocimum tenuiflorum are linalool, alkaloids, ursolic acid, glycosides, carvacrol, tannins, rosmarinic acid, and aromatic compounds, etc. [31, 32].

The plant *Ocimum tenuiflorum* belongs to the Lamiaceae family and is a traditional medicinal plant. It is a culinary herb and an attractive, fragrant ornamental plant known as "*Shyama Tulasi*." The choice of the plant was motivated by the existence of aromatic compounds. The plant contains a variety of phytochemicals such as phenols, flavones, and amino acids and exhibits antimicrobial, antifungal, immune-stimulatory, antistress, antioxidant, and anticarcinogenic activity. It is shown in recent reports that *Ocimum tenuiflorum* exhibits a significant neuroprotective effect and long-term hypoperfusion.

In addition, it is used as an anticonvulsant and anti-inflammatory agent [33, 34]. *Ocimum tenuiflorum*-mediated ZnO nanoparticles are more efficient in inactivating bacterial growth. *Bacillus subtilis, Staphylococcus aureus, and Escherichia coli are pathogenic bacteria. Ocimum tenuiflorum* leaf extract is used as a green mediator for synthesizing ZnO nanocapsules and inactivating bacterial pathogens [35]. Various synthesis methods and results achieved for C-ZnO and G-ZnO are compared and given in Tables 1 and 2. The reason for antibacterial activity against different bacteria is still scanty. It requires more investigation to optimize the size of the nanoparticles, reactive oxygen species (ROS) generation, and stability improvement.

In this work, green synthesis of ZnO nanopowders was achieved using leaf extracts from *the Ocimum tenuiflorum* plant. *Ocimum tenuiflorum* is also called holy basil, tulsi, and Ocimum sanctum. In addition, the structural, surface morphological, optical, and antibacterial activities of ZnO nanopowders have been investigated.

2. Materials and Methods

2.1. Chemical Synthesis Process. Zinc acetate dihydrate (Zn $(CH_3COO)_2$ $2H_2O$) (4 gm) was dissolved in 100 mL of distilled water. The pH value was maintained at 8 by adding sodium hydroxide (NaOH) solution dropwise to the starting solution. The prepared solution was kept under stirring for 2 hours at 80°C using a magnetic stirrer. Once the precipitation is formed in the solution, it is allowed to cool at room temperature for 1 hour to complete the precipitation process. Later, the residue was filtered out and washed several times with DI water and an ethanol (3:1) mixture to eliminate the presence of impurities before being dried at 90°C in the air. Finally, the precipitate was calcined at 400°C for 3 hours to achieve the final product.

2.2. Green Synthesis Process

2.2.1. Preparation of the Leaf Extract. The aqueous extract was made from collected Ocimum tenuiflorum (Tulsi) leaves. About 30 gm of leaves was cleaned adequately in distilled water, chopped into fine pieces, and crushed into 50 ml of distilled water, which was added and heated for about 15 minutes at 60°C-70°C. The crude extracts were then filtered using a Whatman No. 1 filter paper (pore size of

Table 1: Comparison of results and various methods used for the synthesis of C-ZnO.

S.No	Technique	Antibacterial	Ref.
1	Sol-gel	Antibacterial activity increased with a reduction in particle size. GPTMS-modified ZnO NP has demonstrated increased effectiveness.	[36]
2	Chemical method	It has been discovered that the antibacterial activity of goods is closely correlated with the variation in the interaction energy between bacteria and nanoparticles. ROS and oxygen vacancy in well-designed clean and doped ZnO are correlated.	[37]
3	Solution method	Both in the presence of light and the absence of light, surface flaws play a significant role in the generation of ROS.	[38]
4	Surface modification	Surface-modified ZnO samples demonstrated enhanced antibacterial activity and dramatically reduced Zn 2C ion release.	[39]
5	Chemical method	E. coli antimicrobial activity increased.	[40]
6	Solution method	The antibacterial activity of ZnO was unaffected by its crystallographic orientation. *Staphylococcus aureus* was the target of more action than *E. coli*.	[41]
7	Chemical method	Modified ZnO NPs' increased ROS production efficiency, therefore, raises their antibacterial and anticancer properties. ZnO NPs and hybrid ZnO NPs with photo-activated antibacterial and anticancer properties.	[42]
8	Solution method	It is possible to suggest ZnO NP as a potent and efficient antibacterial agent for both Gram-positive and Gram-negative bacteria. ZnO NP treatment caused bacterial cell lysis or explosion, and it had a stronger antibacterial effect on Gram-positive bacteria.	[43]
9	Non-hydrolytic solution route	For S. aureus, *S. typhimurium*, and E. coli, the MIC of ZnO NPs that controls bacterial strain development is determined to be 15 g/ml; however, for K. pneumoniae, it was calculated to be 5 g/ml.	[44]
10	Chemical precipitation	Methicillin-resistant *S. aureus* is resistant to zinc oxide nanoparticles.	[45]

25 mm). Filters with a diameter of 0.6 μm were further refined.

2.2.2. Synthesis of Zinc Oxide Nanopowders. Zinc acetate (Zn $(CH_3COO)_2.2H_2O$) was used as a starting material to prepare 50 mL of an aqueous solution, and an aqueous extract of Ocimum tenuiflorum leaves was employed in the synthesis of G-ZnO NPs. 20 mL of Ocimum tenuiflorum leaf extract was added to a 30 mL aqueous solution of zinc acetate. It was held in a magnetic stirrer at 80°C for one hour. The resulting precipitate was filtered and rinsed several times with water and ethanol (3:1) before being dried in the air at 90°C. The final product was calcined for 3 hours at 400°C. The proposed synthesized mode of ZnO nanopowders is shown in Figure 1.

2.3. Characterizations of ZnO Nanopowders. A PANalytical-PW 340/60 X′ pert PRO X-ray diffractometer was used to study the crystalline structure. X-ray photoelectron spectra (XPS) were analyzed using a Perkin-Elmer PHI 1600 ESCA instrument. Monochromatic Mg Kα radiations (hν = 1486.6 eV) were served for recording. The surface and morphological information of samples were analyzed by using a field emission scanning electron microscope (FE-SEM) (Make and Model: Hitachi SU8000). A transmission electron microscope (TEM) (Make and Model: Hitachi H-7100) was used to investigate the structural entities of nanoparticles. EDAX (energy dispersive X-ray analysis) was used to perform the elemental studies (Model: JEOL-JSM 6390 with attachment INCA-Penta FETX3 OXFORD). A spectrofluorometer (Jobin YVon Inc. FLUROLOG-FL3-11) was used to observe photoluminescence (PL) spectra with a 450 W xenon lamp as the excitation source at 325 nm. A Shimadzu UV-2500 spectrophotometer was also used to produce diffuse reflectance spectra in the wavelength range of 300–2000 nm. TGA/DTG studies were recorded using a Perkin-Elmer diamond instrument in the temperature range of 30–1000°C.

2.4. Antibacterial Activity Evaluation of ZnO Nanopowders. The antibacterial behavior of the synthesized ZnO nanopowders was investigated using the agar well diffusion method against *Escherichia coli* (E.*coli*) and *Staphylococcus aureus* (*S. aureus*) bacteria. Mueller–Hinton broth was utilized as a nutrient agar medium for bacterial growth. Four wells, each with a diameter of 5 mm, were drilled, and 200 g/mL of the sample solution was poured into each well. The inhibitory zone was measured by millimeters after 24 hours of incubation at 37°C. The control substance was dimethyl sulfoxide (DMSO).

3. Results and Discussion

3.1. Crystalline Structure Analysis. Figure 2 shows an X-ray diffractogram of C-ZnO nanopowders and G-ZnO nanopowders. All diffraction lines match the Joint Committee on Powder Diffraction Standards (JCPDS) file standard pattern (card No: 36–1451), indicating that the material obtained by green synthesis is ZnO nanopowders. The crystallite size (D) is calculated using the following formula [56]:

Table 2: Comparison of results and various methods used for the synthesis of G-ZnO.

S.No	Technique	Findings	Ref.
1	Using solanum nigrum leaf extract	The antibacterial properties of the synthesized NPs were investigated against both Gram-positive (*S. aureus*) and Gram-negative (S. Paratyphi, V. cholerae, and *E. coli*) bacteria.	[46]
2	Anisochilus carnosus leaf extract mediated	Green ZnO NPs produced using leaf extract and solvent displayed a more pronounced significant zone of inhibition.	[47]
3	1-Butyl-3-methylimidazolium bis(trifluoromethylsulfonyl) imide, (bmim) [NTf2] as a green solvent.	Strong antibacterial activity against *E. coli* is produced when ZnO nanofluid concentrations are increased.	[48]
4.	Orange fruit peel extract	Without UV light, ZnO NPs demonstrated strong antibacterial action against *E. coli* and *S. aureus*. The bactericidal properties of talc. With regard to the synthesis parameters, S. aureus varied widely.	[49]
5	Beta vulgaris, Cinnamomum tamala, Cinnamomum verum, brassica oleracea var. italica were used for green synthesis	Using fungal stains for Candida albicans and Aspergillus Niger, ZnO NPs' antifungal activity was also demonstrated. It was discovered that ZnO NPs made with Beta vulgaris were active against *A. niger*, whereas those made with Cinnamomum tamala were active against albicans. Furthermore, ZnO NPs are made from the extract of Brassica oleracea var. italica that has demonstrated efficacy against both fungal stains.	[50]
6	*Silybum marianum L* seed extract	ZnO samples were tested against *E. coli* to determine whether they may be used as antibacterial agents.	[51]
7	*Fusarium keratoplasticum* strain (A1-3) and Aspergillus niger strain (G3-1) were used for the synthesis of ZnO NPs.	Exhibited a better UV protection index and antibacterial capabilities against harmful microorganisms than hexagonal ZnO NPs. Shape-dependent biocidal activity of NPs was demonstrated by antibacterial activities against Gram-negative and Gram-positive bacteria as well as in vitro cytotoxicity against three different animal cell lines.	[52]
8	*Euphorbia* hirta leaf extract	Performed well against *S. aureus*	[53]
9	Dysphania ambrosioides extract	Aggregatibacter actinomycetemcomitans, Porphyromonas gingivalis, Prevotella intermedia, Streptococcus mutans, and streptococcus sanguinis are among the bacteria commonly found in human mouths and are linked to dental conditions. *Staphylococcus aureus*, Staphylococcus epidermidis, Escherichia coli, and Pseudomonas aeruginosa.	[54]
10	*Bauhinia* tomentosa leaf	Compared to Gram-positive bacteria, ZnO NPs had significantly more antibacterial action against Gram-negative pathogens *P. aeruginosa* and *E. coli*. The study's findings showed that B. tomentosa leaf extract, which contains phytochemicals like alkaloids, terpenoids, flavonoids, tannins, carbohydrates, and sterols, has the ability to bio reduce zinc oxide and that the ZnO NPs produced can be used effectively as a more effective bactericidal agent in biological applications.	[55]

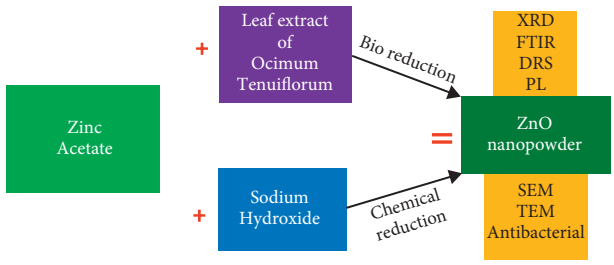


Figure 1: Synthesis process overview.

$$D = \frac{0.9\lambda}{\beta \cos \theta}, \quad (1)$$

where 'λ, β, and θ' are the wavelengths of X-ray used, full-width at half-maximum, and Bragg's angle, respectively [57]. The crystallite size of the C-ZnO nanopowder is 58 nm, whereas G-ZnO nanopowders exhibit 6 nm. The crystallite size reduction is also influenced by the biomolecules present in the plant extract, and it is supported by improving the oxygen process in the ZnO lattice. Gunalan et al. suggested that the decrease in crystallite size may be due to the kind of plant extract along with the temperature of oxide formation [58, 59].

3.2. X-Ray Photoelectron Spectra. XPS spectra of C-ZnO and G-ZnO confirmed that the indexed peaks could be endorsed to Zn, O, and C, as illustrated in Figure 3. The mentioned carbon element is from pump oil in the vacuum system of the XPS instrument. The binding energy is calibrated by taking the carbon C1 peak (284.8 eV) as a reference. The peaks at 1021.4 eV and 1044.6 eV were ascertained to be the binding energy of Zn 2p3/2 and Zn 2p1/2 states in the ZnO lattice. Through this confirmation, we could conclude that there are no other peaks in both samples. Hence, purity of the samples was verified.

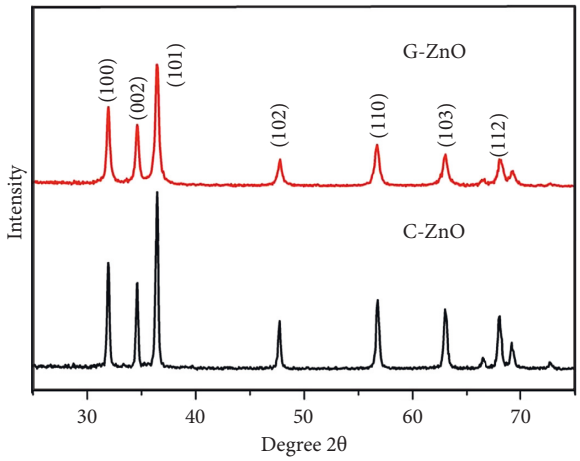


Figure 2: XRD peaks of C-ZnO and G-ZnO nanopowders.

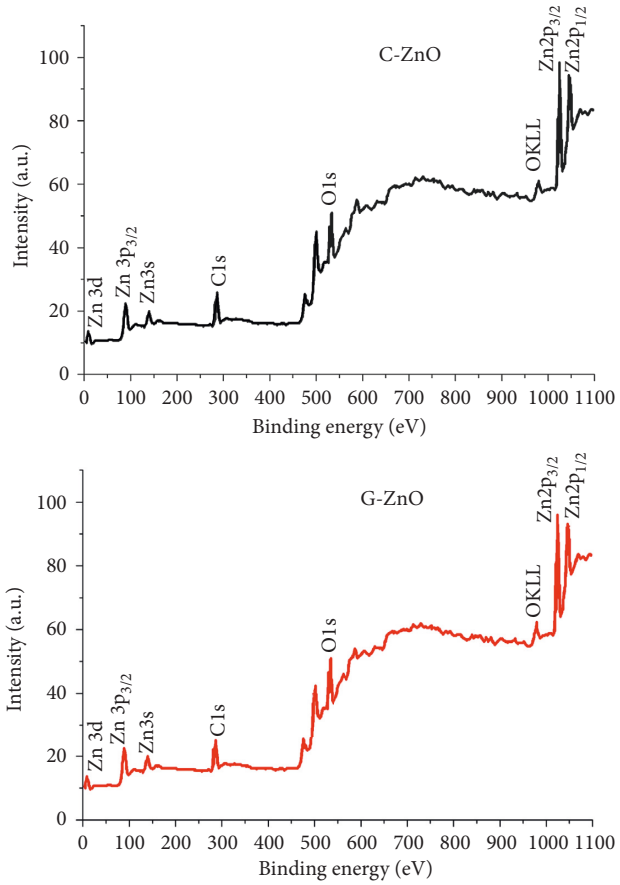


Figure 3: XPS spectra of C-ZnO and G-ZnO nanopowders.

3.3. FTIR Analysis. FTIR is employed as a confirmation technique for nanoparticle formation, providing an impression of existing molecules' vibrational and rotational modes. It is also commonly used to identify functional and potential phytochemical compounds in reducing and stabilizing ZnO nanopowders. Figure 3 represents the FTIR spectra of ZnO nanopowders. From this spectrum, the chemically and greenery synthesized ZnO nanopowders show a broad peak around 3415 cm^{-1} for the stretching vibration of the O–H bond [60].

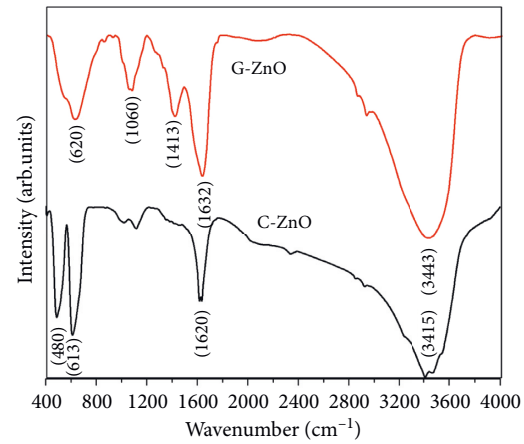


Figure 4: FTIR spectra of C-ZnO and G-ZnO nanopowders.

A sharp peak received around 1620 cm^{-1} is assigned to H–O–H bending vibration and is transferred to a small amount of H_2O in ZnO nanocrystals [61]. The peaks received near 1413 cm^{-1} were considered carboxyl assembly [62]. Stretching amine endorsed the peak at 1060 cm^{-1} [63]. The reduction of zinc ions to ZnO nanopowders was aided by these compounds, particularly flavonoids and other phenolics. The characteristic absorption of the Zn–O bond is reflected from 480 to 620 cm^{-1} [64]. The alteration in intensity, band position, and FWHM authenticate the subsistence of defect states.

3.4. Surface Morphology and Elemental Analysis. As seen in the FESEM images, C-ZnO nanopowders have nonagglomerated particles in the 70–90 nm range, whereas G-ZnO nanopowders have small particles in the 10–20 nm range, as shown in Figure 4. The size of the nanoparticles might be reduced due to the addition of plant extract. The antibacterial property seems to be mostly dependent on particle size reduction. Figure 5 shows the TEM images of C-ZnO and G-ZnO nanopowders. It is visible in hexagonal-shaped morphologies. The TEM micrograph strongly supports the particle size of C-ZnO and G-ZnO nanopowders, respectively. The presence of elements like Zn and O is confirmed through the EDAX profile (Figure 5). The elemental copmosition of C-ZnO and G-ZnO is given as (Zn = 46.38 at. wt.%, O = 53.62 at.wt.%) and (Zn = 49.69 at. wt.%, O = 50.31 at.wt.%), respectively. The lowest presence of oxygen in G-ZnO evidenced the existence of oxygen vacancies.

3.5. Optical Studies. As seen in the FESEM images, C-ZnO nanopowders have nonagglomerated particles in the 70–90 nm range, whereas G-ZnO nanopowders have small particles in the 10–20 nm range, as shown in Figure 4. The size of the nanoparticles might be reduced due to the addition of plant extract. The antibacterial property seems to be mostly dependent on particle size reduction. Figure 5 shows the TEM images of C–ZnO and G-ZnO nanopowders. It is visible in hexagonal-shaped morphologies. The TEM micrograph strongly supports

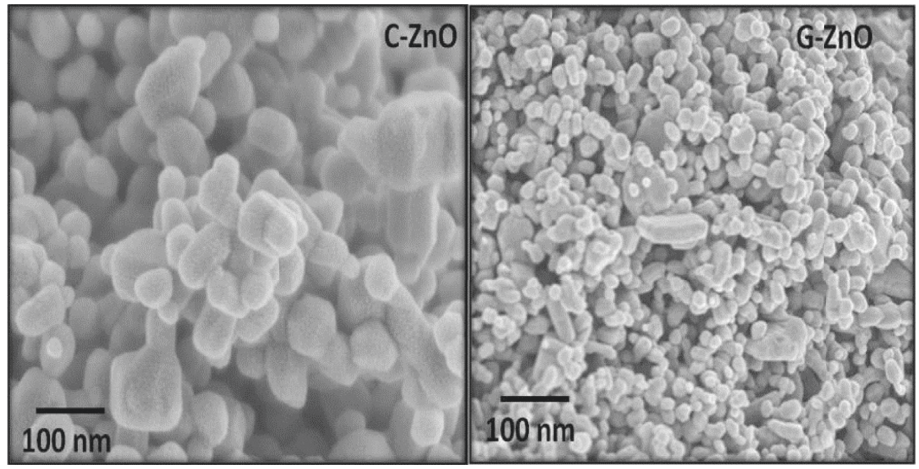


Figure 5: SEM images of C-ZnO and G-ZnO nanopowders.

the particle size of C–ZnO and G-ZnO nanopowders, respectively. The presence of elements like Zn and O is confirmed through the EDAX profile (Figure 5). In C–ZnO (Zn = 46.38 at. wt. %, O = 53.62 at.wt.%), G-ZnO (Zn = 49.69 at. wt. %, O = 50.31 at.wt.%).The lowest presence of oxygen in G-ZnO evidenced the existence of oxygen vacancies [32].

$$\alpha h\nu = A\left(h\nu - E_g\right)^{1/2}, \tag{2}$$

where α is the absorption coefficient, A is the constant, $h\nu$ is the incident photons' energy, Eg is the band gap energy in eV, and $n = 1/2$ (for direct allowed transitions). Tauc's plot is shown in Figure 6. The band gap values varied from 3.28 to 3.33 eV for C-ZnO and G-ZnO nanopowders. This band gap variation is ascertained in the interpretation of nanoparticle size.

Figure 7 shows the PL spectra of C-ZnO and G-ZnO nanopowders. The near band edge (NBE) emission shows the band-to-band transition of electrons, which was accompanied by the peak at 395 nm [65]. The prominent emission peak at 424 nm was due to zinc interstitial, while the weak emission peak at 450 nm was due to zinc vacancies. Because of singly ionized oxygen vacancy, the emission peak at 468 nm has formed [66]. The type of plant extract may be responsible for the peak intensity at 468 nm of G-ZnO nanopowders. The formation of hydroxyl radicals by these singly ionized oxygen vacancies improves the antibacterial activity of produced ZnO nanopowders.

Green synthesized ZnO nanoparticles showed a distinct electronic and optical behavior since they possess an exciton quantum confinement phenomenon. The exciton Bohr radius is the comparable size of nanoparticles. ZnO nanoparticles may behave as quantum dots that can absorb small wavelengths with the ability to emit longer wavelengths in the visible region. Photoluminescence spectra favored the biological synthesis of semiconducting ZnO nanoparticles, and these nanoparticles exhibited exciton quantum confinement and stability in an aqueous medium [67].

3.6. Antibacterial Activity. The antimicrobial activities of ZnO nanoparticles in contact with bacteria and fungi are shaped by particle sizes, morphologies, and specific surface areas. Manuela Stan et al. observed the antibacterial activities of plant extracts, such as *Allium sativum*, *Rosmarinus officinalis*, and *Ocimum basilicum* [68]. Their study results show that green synthesized ZnO nanoparticles exhibit intense levels of bactericidal activities against *S. aureus*, *B. subtilis*, *E. coli*, and *Salmonella typhimurium* strains. We also found that biosynthesized zinc oxide nanoparticles obtained from *Costus pictus* leaf extract exhibit good antibacterial behavior.

We also found that biosynthesized zinc oxide nanoparticles obtained from *Ocimum tenuiflorum* leaf extract exhibit good antibacterial behavior [69].

Using the agar well diffusion method, the antibacterial activities of C-ZnO and G-ZnO nanopowders against two different bacterial strains, *S. aureus* ($G+$ve) and *E.coli* (G-ve), were examined. The G-ZnO (22 mm) sample has better antibacterial activity than the C–ZnO (18 nm) sample, according to the results (Figure 8). There is no inhibition zone around the control (C). The size of the nanoparticles may be responsible for the increased antibacterial activity of G-ZnO powders. The following eqautions are given to explain about the mechanism of ROS production and the role of electrons on the process [70].

The capacity of these ROS to break cell membranes and kill bacteria is well recognized.

$$\begin{aligned}
G - Zn - O + h\nu &\longrightarrow e^- + h^+,\\
h^+ + H_2O &\longrightarrow H^+ + {}^{\bullet}OH,\\
e^- + O_2^{\bullet} &\longrightarrow O_2^{\bullet -},\\
O_2^{\bullet} + H^+ &\longrightarrow HO_2^{\bullet},\\
HO_2^{\bullet} + e^- &\longrightarrow HO_2^{\bullet -},\\
HO_2^{\bullet -} + H^+ &\longrightarrow H_2O_2.
\end{aligned} \tag{3}$$

ZnO nanoparticles can produce ROS in water suspensions, and ROS are responsible for the inhibitory effect on the growth of bacteria [71]. ROS such as •OH, $O_2^{\bullet -}$, and H_2O_2 are produced by transferring electrons from VB to CB. The most active •OH is obtained from the oxidation process.

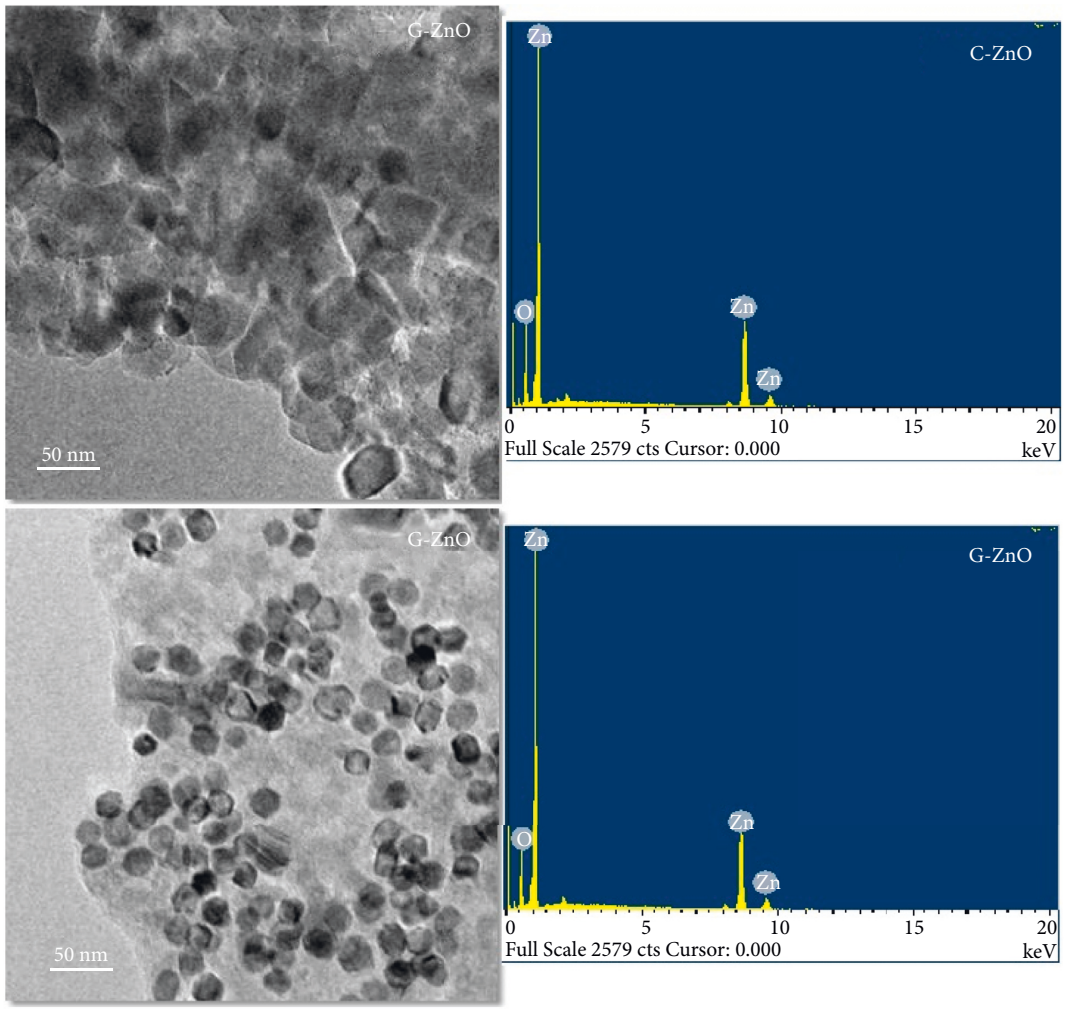


Figure 6: TEM images and EDAX spectra of C-ZnO and G-ZnO nanopowders.

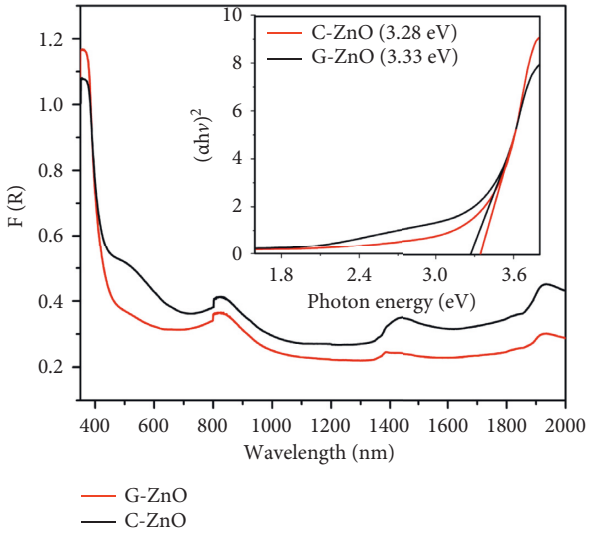


Figure 7: Diffuse reflectance spectra and band gap value of C-ZnO and G-ZnO nanopowders.

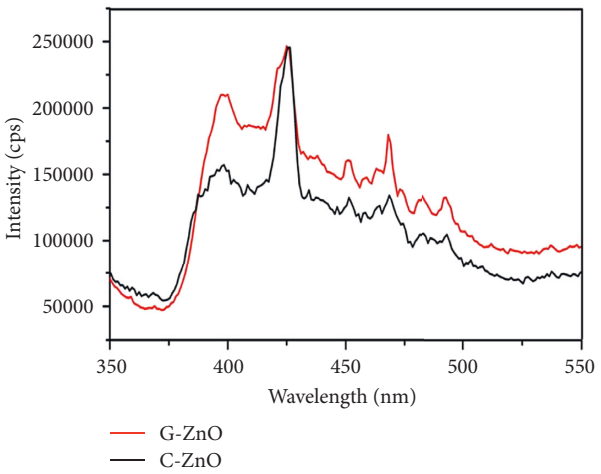


Figure 8: PL spectra of C-ZnO and G-ZnO nanopowders.

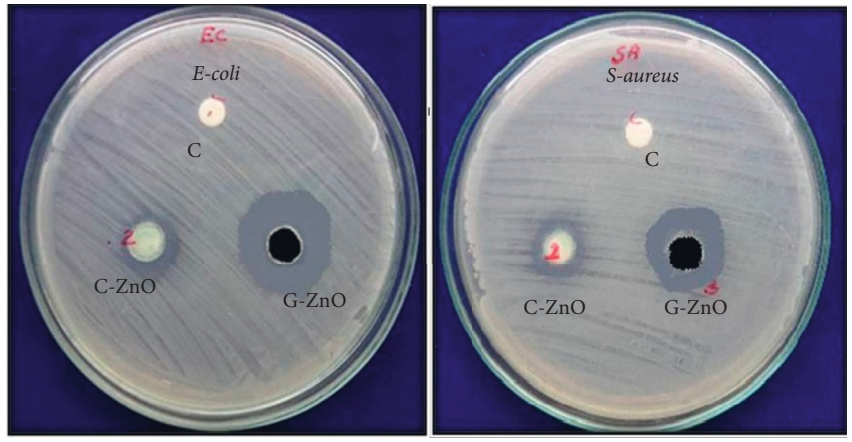


Figure 9: Antibacterial activity of C–ZnO and G-ZnO nanopowders.

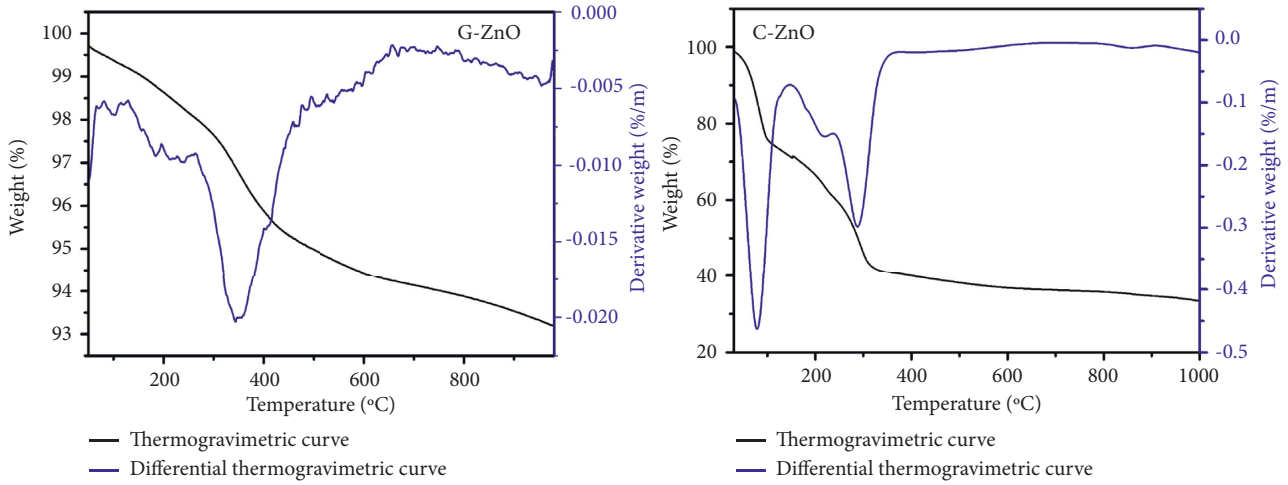


Figure 10: Thermogravimetric analysis of C-ZnO and G-ZnO nanopowders.

H_2O_2 and the hydroxyl radical (•OH) were powerful oxidizing agents to prevent the growth of bacterial cells and introduce heavy toxicity to bacteria. ROS accelerate the disintegration of the cell wall and consequently the leakage of cell elements and ultimately cell death.

Superoxide anions and hydroxyl radicals ($^{\bullet}$OH) are negatively charged. As a result, they cannot get through the cell membrane but can harm the bacterial surface, whereas hydrogen peroxide (H_2O_2) can get right through the cell wall and kill the bacterium [72]. In this study, the number of singly ionized oxygen vacancies is evidenced by the PL spectra, which are responsible for ROS generation.

G-ZnO has the highest bacterial killing capacity because of the enhanced crystallite size and high density of oxygen vacancies, which show the way to higher values of ROS [73]. Furthermore, G-ZnO nanopowders exhibit a higher antibacterial efficacy against Gram-negative (G-) bacteria than against Gram-positive (*G*+) bacteria. The following explains why this happened: *G*+ bacteria often have a solid thick cell wall with many lipoteichoic acids (LTAs) and other components like peptidoglycan. G-bacteria, conversely, have fragile cell walls but a complicated cell wall structure. Polysaccharides, lipids, and proteins are abundant in the outer membrane. Outside the core membrane, there is also an open area called the periplasmic region, followed by a thin layer of peptidoglycan encircled by another membrane. As a result, unlike *G*+ bacteria, the cell membrane of G-bacteria cannot be easily destroyed. Therefore, even though *G*+ bacteria have very high, thicker cell walls, their less negative nature allows a lot of negatively charged free radicals to penetrate the cell wall, inflicting significant damage. This suggests that plant extracts' phytochemical products strongly affect the cell walls of bacteria.

Smaller nanoparticles can also easily pass through cell membranes, allowing increased contact area for the chemical to react with microorganisms. In addition, green synthesis reduces particle size, as indicated by FESEM and TEM data, and a further size reduction is observed. This reduction in particle size has an impact on the antibacterial activity of the G-ZnO samples. The antibacterial activity is enhanced due to the smaller size of the ZnO nanoparticles. It was already reported that ZnO NPs might damage the bacterial cell membrane, resulting in the lysis of intracellular contents and

ultimately proving to be lethal for the bacterial cell (Citation given). The thickness of the cell wall of Gram-positive bacteria is due to the presence of the peptidoglycan layer. The stability of antibacterial activity for C-ZnO and G-ZnO NPs is discussed. The more prominent inhibition was observed against *E.coli bacteria* for G-ZnO NPs.

3.7. Thermal Analysis. TGA and DTG analyses were carried out in the standard atmosphere for the temperature ranges from 30 to 1000°C to understand the changes occurring during the heat treatment of as-prepared C–ZnO. TGA and DTG curves are shown in Figure 9 and 10, and they reveal two-step gravimetric changes, which indicate the occurrence of weight loss at two stages during the heat treatment. The initial weight loss occurring in the temperature range of 30 to 100°C can be attributed to the vaporization of water molecules from the prepared sample [74]. The second gravimetric change in the field of 100 to 300°C corresponds to another weight loss associated with the thermal decomposition of Zn $(OH)_2$ to ZnO NPs [75]. Beyond the temperature of 300°C, there is a slight decrease in the weight, which may be due to the exothermic reaction-assisted oxygen desorption from ZnO [76]. The temperature range of the endothermic peak in the DTG curve matches well with that of weight loss in the TGA curve. Hence, from TGA and DTG analysis, the temperature of 300°C is considered the minimum suitable temperature for different calcination processes. We ensure there is always a space between the number and degree symbol.

4. Conclusion

C-ZnO and G-ZnO nanopowders have been effectively synthesized using a simple soft chemical route and a green synthesis method. The results of the X-ray diffraction pattern revealed that the synthesized nanopowders have a hexagonal wurtzite structure. The synthesized nanocrystallite size was decreased more due to the incorporation of Ocimum tenuiflorum leaf extract. The zinc acetate was reduced to ZnO due to the incorporation of leaf extract. The TGA/DTG analysis evidenced the thermal behaviors of ZnO nanoparticles. The optical band gap value varies from 3.28 to 3.33 eV. G-ZnO nanopowders exhibit excellent antibacterial activities than C-ZnO. From investigations, it is concluded that the plant extract added to ZnO nanopowders causes the generation of ROS, which is responsible for increasing antibacterial efficiencies. The improved antibacterial efficacy may be suitable for removing bacterial pollution from water. It is the best platform for nanopowder synthesis because it is free of toxic chemicals and has enhanced antibacterial properties. The stability of ROS generation and the particle size will be optimized in future work. Then, Hence, it is suggested that the G-ZnO NPs shall be utilized to react against the trageted bacteria.

Data Availability

The data used to support the findings of this study are available from the corresponding author upon request.

Conflicts of Interest

The authors declare that they have no conflicts of interest.

References

[1] C. Belkhaoui, N. Mzabi, H. Smaoui, and P. Daniel, "Enhancing the structural, optical and electrical properties of ZnO nanopowders through (Al + Mn) doping," *Results in Physics*, vol. 12, pp. 1686–1696, 2019.

[2] A. Becheri, M. Durr, P. Lo Nostro, and P. Baglioni, "Synthesis and characterization of zinc oxide nanoparticles: application to textiles as UV-absorbers," *Journal of Nanoparticle Research*, vol. 10, no. 4, pp. 679–689, 2007.

[3] W. W. Guo, T. Liu, W. Zeng, D. Liu, Y. Chen, and Z. Wang, "Gas-sensing property improvement of ZnO by hierarchical flower-like architectures," *Materials Letters*, vol. 65, no. 23-24, pp. 3384–3387, 2011.

[4] P. Visali and R. Bhuvaneswari, "Photoluminescence and enhanced photocatalytic activity of ZnO nanoparticles through incorporation of metal dopants Al and Ca," *Optik*, vol. 202, Article ID 163706, 2020.

[5] C. A. S-Robles, O. Nava, L. Cornejo et al., *Journal of Molecular Structure*, vol. 1225, Article ID 129101, 2021.

[6] S. Yılmaz, M. Parlak, Ş. Özcan, M. Altunbas, E. McGlynn, and E. Bacaksız, "Structural, optical and magnetic properties of Cr doped ZnO microrods prepared by spray pyrolysis method," *Applied Surface Science*, vol. 257, no. 22, pp. 9293–9298, 2011.

[7] H. Yang, C. Zhang, X. Shi et al., "Water-soluble superparamagnetic manganese ferrite nanoparticles for magnetic resonance imaging," *Biomaterials*, vol. 31, no. 13, pp. 3667–3673, 2010.

[8] Y. Wang, Q. Zhao, N. Han et al., "Mesoporous silica nanoparticles in drug delivery and biomedical applications," *Nanomedicine: Nanotechnology, Biology and Medicine*, vol. 11, no. 2, pp. 313–327, 2015.

[9] B. Abebe, E. A. Zereffa, A. Tadesse, and H. C. A. Murthy, "A review on enhancing the antibacterial activity of ZnO: mechanisms and microscopic investigation," *Nanoscale Research Letters*, vol. 15, no. 1, p. 190, 2020.

[10] B. Lallo da Silva, B. L. Caetano, B. G. Chiari-Andréo, R. C. L. R. Pietro, and L. A. Chiavacci, "Increased antibacterial activity of ZnO nanoparticles: influence of size and surface modification," *Colloids and Surfaces B: Biointerfaces*, vol. 177, pp. 440–447, 2019.

[11] S. Anitha and S. Muthukumaran, "Structural, optical and antibacterial investigation of La, Cu dual doped ZnO nanoparticles prepared by co-precipitation method," *Materials Science and Engineering: C*, vol. 108, Article ID 110387, 2020.

[12] R. Karthick, P. Sakthivel, C. Selvaraju, and M. S. Paulraj, "Tuning of photoluminescence and antibacterial properties of ZnO nanoparticles through Sr doping for biomedical applications," *Journal of Nanomaterials*, vol. 2021, Article ID 8352204, 7 pages, 2021.

[13] M. G. Nair, M. Nirmala, K. Rekha, and A. Anukaliani, "Structural, optical, photo catalytic and antibacterial activity of ZnO and Co doped ZnO nanoparticles," *Materials Letters*, vol. 65, no. 12, pp. 1797–1800, 2011.

[14] R. Saleh, N. F. Djaja, and S. P. Prakoso, "The correlation between magnetic and structural properties of nanocrystalline transition metal-doped ZnO particles prepared by the co-precipitation method," *Journal of Alloys and Compounds*, vol. 546, pp. 48–56, 2013.

[15] K. Saravanakumar, R. K. Sankaranarayanan, P. Sakthivel, and K. C. S. Pushpa, "Microwave assisted green synthesis of zinc oxide nanoparticles for biological applications," *PROCEEDINGS OF ADVANCED MATERIAL, ENGINEERING & TECHNOLOGY*, vol. 2270, Article ID 110003, 2020.

[16] S. Chakraborty, C. Sb. Tiwary, A. K. Kole, P. Kumbhakar, and K. Chattopadhyay, "A simple method of synthesis and optical properties of Mn doped ZnO nanocups," *Materials Letters*, vol. 91, pp. 379–382, 2013.

[17] B. R. . Nityasree, R. K. Chalannavar, S. Kouser et al., *Advances in Natural Sciences: Nanoscience and Nanotechnology*, vol. 12, Article ID 015009, 2021.

[18] R. Dobrucka and J. Dugaszewska, *Saudi Journal of Biological Sciences*, vol. 23, p. 517, 2016.

[19] M. S. Saif, A. Zafar, M. Waqas et al., "Phyto-reflexive Zinc Oxide Nano-Flowers synthesis: an advanced photocatalytic degradation and infectious therapy," *Journal of Materials Research and Technology*, vol. 13, pp. 2375–2391, 2021.

[20] M. Hasan, M. Altaf, A. Zafar et al., "Bioinspired synthesis of zinc oxide nano-flowers: a surface enhanced antibacterial and harvesting efficiency," *Materials Science and Engineering: C*, vol. 119, Article ID 111280, 2021.

[21] M. Hasan, Z. Teng, J. Iqbal et al., *Nanoscience and Nanotechnology Letters*, 2013.

[22] R. S. Varma, "Greener approach to nanomaterials and their sustainable applications," *Current Opinion in Chemical Engineering*, vol. 1, no. 2, pp. 123–128, 2012.

[23] J. Virkutyte and R. S. Varma, "Green synthesis and nanomaterials: environmental aspects," in *Sustainable Nanotechnology and the Environment: Advances and Achievements, ACS Symposium Series 1124*, N. Shamin and V. K. Sharma, Eds., American Chemical Society, Oxford University Press, Washington, DC, USA, 2013.

[24] C. J. Li, "Reflection and perspective on green chemistry development for chemical synthesis—daoist insights," *Green Chemistry*, vol. 18, no. 7, pp. 1836–1838, 2016.

[25] K. H. Sudheer Kumar, N. Dhananjaya, and L. S. Reddy, *Journal of Science: Adv. Mater. Devices*, vol. 3, p. 303, 2018.

[26] K. Kanagamani, P. Muthukrishnan, A. Kathiresan, K. Shankar, P. Sakthivel, and M. Ilayaraja, "Detoxication and theranostic aspects of biosynthesised zinc oxide nanoparticles for drug delivery," *Acta Metallurgica Sinica*, vol. 34, no. 5, pp. 729–740, 2021.

[27] M. Gupta, R. S. Tomar, S. Kaushik, R. K. Mishra, and D. Sharma, "Effective antimicrobial activity of green ZnO nano particles of catharanthus roseus," *Frontiers in Microbiology*, vol. 9, p. 2030, 2018.

[28] A. Taşdemir, N. Akman, A. Akkaya, R. Aydın, and B. Şahin, "Green and cost-effective synthesis of zinc oxide thin films by L-ascorbic acid (AA) and their potential for electronics and antibacterial applications," *Ceramics International*, vol. 48, no. 7, Article ID 10164, 2022.

[29] M. Naseer, U. Aslam, B. Khalid, and B. Chen, "Green route to synthesize Zinc Oxide Nanoparticles using leaf extracts of Cassia fistula and Melia azadarach and their antibacterial potential," *Scientific Reports*, vol. 10, no. 1, p. 9055, 2020.

[30] B. Şahin, S. Soylu, M. Kara, M. Türkmen, R. Aydin, and H. Çetin, "Superior antibacterial activity against seed-borne plant bacterial disease agents and enhanced physical properties of novel green synthesized nanostructured ZnO using Thymbra spicata plant extract," *Ceramics International*, vol. 47, no. 1, pp. 341–350, 2021.

[31] H. A. Rafaie, N. A. Samat, and R. M. Nor, "Effect of pH on the growth of zinc oxide nanorods using Citrus aurantifolia extracts," *Materials Letters*, vol. 137, pp. 297–299, 2014.

[32] N. J. Sushma, B. Mahitha, K. Mallikarjuna, and B. D. P. Raju, "Bio-inspired ZnO nanoparticles from Ocimum tenuiflorum and their in vitro antioxidant activity," *Applied Physics*, vol. 122, no. 5, p. 544, 2016.

[33] D. Philip and C. Unni, "Extracellular biosynthesis of gold and silver nanoparticles using Krishna tulsi (Ocimum sanctum) leaf," *Physica E: Low-Dimensional Systems and Nanostructures*, vol. 43, no. 7, pp. 1318–1322, 2011.

[34] N. Ahmad, S. Sharma, M. K. Alam et al., "Rapid synthesis of silver nanoparticles using dried medicinal plant of basil," *Colloids and Surfaces B: Biointerfaces*, vol. 81, no. 1, pp. 81–86, 2010.

[35] S. U. Yanpallewar, S. Rai, M. Kumar, and S. B. Acharya, "Evaluation of antioxidant and neuroprotective effect of on transient cerebral ischemia and long-term cerebral hypoperfusion," *Pharmacology Biochemistry and Behavior*, vol. 79, no. 1, pp. 155–164, 2004.

[36] B. Lallo da Silva, B. L. Caetano, B. G. Chiari-Andréo, R. C. L. R. Pietro, and L. A. Chiavacci, "Increased antibacterial activity of ZnO nanoparticles: influence of size and surface modification," *Colloids and Surfaces B: Biointerfaces*, vol. 177, pp. 440–447, 2019.

[37] V. L. Prasanna and R. Vijayaraghavan, "Chemical manipulation of oxygen vacancy and antibacterial activity in ZnO," *Materials science & engineering. C, Materials for biological applications*, vol. 77, pp. 1027–1034, 2017.

[38] V. Lakshmi Prasanna and R. Vijayaraghavan, "Insight into the mechanism of antibacterial activity of ZnO: surface defects mediated reactive oxygen species even in the dark," *Langmuir*, vol. 31, no. 33, pp. 9155–9162, 2015.

[39] Y. H. Leung, C. M. N. Chan, A. M. C. Ng et al., "Antibacterial activity of ZnO nanoparticles with a modified surface under ambient illumination," *Nanotechnology*, vol. 23, no. 47, Article ID 475703, 2012.

[40] Y. Liu, L. He, A. Mustapha, H. Li, Z. Q. Hu, and M. Lin, "Antibacterial activities of zinc oxide nanoparticles against *Escherichia coli* O157:H7," *Journal of Applied Microbiology*, vol. 107, no. 4, pp. 1193–1201, 2009.

[41] T. Ohira, O. Yamamoto, Y. Iida, and Z. e Nakagawa, "Antibacterial activity of ZnO powder with crystallographic orientation," *Journal of Materials Science: Materials in Medicine*, vol. 19, no. 3, pp. 1407–1412, 2008.

[42] P. Sivakumar, M. Lee, Y. S. Kim, and M. S. Shim, "Photo-triggered antibacterial and anticancer activities of zinc oxide nanoparticles," *Journal of Materials Chemistry B*, vol. 6, no. 30, pp. 4852–4871, 2018.

[43] A. A. Tayel, W. F. El-Tras, S. Moussa et al., *Journal of Food Safety*, vol. 31, p. 211, 2011.

[44] R. Wahab, A. Mishra, S.-Il Yun, Y.-S. Kim, and H.-S. Shin, "Antibacterial activity of ZnO nanoparticles prepared via non-hydrolytic solution route," *Applied Microbiology and Biotechnology*, vol. 87, no. 5, pp. 1917–1925, 2010.

[45] U. Kadiyala, E. S. Turali-Emre, J. H. Bahng, N. A. Kotov, and J. S. VanEpps, "Unexpected insights into antibacterial activity of zinc oxide nanoparticles against methicillin resistant-*Staphylococcus aureus*(MRSA)," *Nanoscale*, vol. 10, pp. 4927–4939, 2018.

[46] M. Ramesh, M. Anbuvannan, and G. Viruthagiri, "Green synthesis of ZnO nanoparticles using Solanum nigrum leaf extract and their antibacterial activity," *Spectrochimica Acta Part A: Molecular and Biomolecular Spectroscopy*, vol. 136, pp. 864–870, 2015.

[47] M. Anbuvannan, M. Ramesh, G. Viruthagiri, N. Shanmugam, and N. Kannadasan, "Anisochilus carnosus leaf extract mediated synthesis of zinc oxide nanoparticles for antibacterial and photocatalytic activities," *Materials Science in Semiconductor Processing*, vol. 39, pp. 621–628, 2015.

[48] R. Jalal, E. K. Goharshadi, M. Abareshi, M. Moosavi, A. Yousefi, and P. Nancarrow, "ZnO nanofluids: green synthesis, characterization, and antibacterial activity," *Materials Chemistry and Physics*, vol. 121, no. 1-2, pp. 198–201, 2010.

[49] T. U. Doan Thi, T. T. Nguyen, Y. D. Thi, K. H. Ta Thi, B. T. Phan, and K. N. Pham, "Green synthesis of ZnO nanoparticles using orange fruit peel extract for antibacterial activities," *RSC Advances*, vol. 10, no. 40, pp. 23899–23907, 2020.

[50] A. M. Pillai, V. S. Sivasankarapillai, A. Rahdar et al., "Green synthesis and characterization of zinc oxide nanoparticles with antibacterial and antifungal activity," *Journal of Molecular Structure*, vol. 1211, Article ID 128107, 2020.

[51] F. M. Arvanag, A. Bayrami, A. H. Yangjeh, and S. R. Pouran, *Materials Science and Engineering: C*, vol. 97, p. 397, 2019.

[52] A. A. Mohamed, A. Fouda, M. Ali Abdel-Rahman et al., *Biocatalysis and Agricultural Biotechnology*, vol. 19, Article ID 101103, 2019.

[53] W. Ahamed and D. Kalra, *J. King Saud Univ. Eng. Sci.*vol. 32, p. 2358, 2020.

[54] R. Á-Chimal, V. I. G. Pérez, M. A. Á-Pérez, and J. Á. A-Alatorre, *Materials Science and Engineering: C*, vol. 118, Article ID 111540, 2021.

[55] G. Sharmila, C. Muthukumaran, K. Sandiya et al., "Biosynthesis, characterization, and antibacterial activity of zinc oxide nanoparticles derived from Bauhinia tomentosa leaf extract," *Journal of Nanostructure in Chemistry*, vol. 8, no. 3, pp. 293–299, 2018.

[56] S. Sharma, K. Kumar, N. Thakur, and M. S. Chauhan, "Ocimum tenuiflorum leaf extract as a green mediator for the synthesis of ZnO nanocapsules inactivating bacterial pathogens," *Chemical Papers*, vol. 74, no. 10, pp. 3431–3444, 2020.

[57] K. Saravanakumar, P. Sakthivel, and R. K. Sankaranarayanan, "Influence of Sn4+ ion on band gap tailoring, optical, structural and dielectric behaviors of ZnO nanoparticles," *Spectrochimica Acta Part A: Molecular and Biomolecular Spectroscopy*, vol. 267, Article ID 120487, 2022.

[58] S. Gunalan, R. Sivaraj, and V. Rajendran, "Green synthesized ZnO nanoparticles against bacterial and fungal pathogens," *Progress in Natural Science: Materials International*, vol. 22, no. 6, pp. 693–700, 2012.

[59] K. P. Shinde, R. C. Pawar, B. B. Sinha, H. S. Kim, S. S. Oh, and K. C. Chung, *Ceramics International*, vol. 40, Article ID 16799, 2014.

[60] S. Qasim, A. Zafar, M. S. Saif et al., "Green synthesis of iron oxide nanorods using Withania coagulans extract improved photocatalytic degradation and antimicrobial activity," *Journal of Photochemistry and Photobiology B: Biology*, vol. 204, Article ID 111784, 2020.

[61] K. R. Ahammed, M. Ashaduzzaman, S. C. Paul et al., "Microwave assisted synthesis of zinc oxide (ZnO) nanoparticles in a noble approach: utilization for antibacterial and photocatalytic activity," *SN Applied Sciences*, vol. 2, no. 5, p. 955, 2020.

[62] S. Muthukumaran and R. Gopalakrishnan, "Structural, FTIR and photoluminescence studies of Cu doped ZnO nanopowders by co-precipitation method," *Optical Materials*, vol. 34, no. 11, pp. 1946–1953, 2012.

[63] Y. A. Selim, M. A. Azb, I. Ragab, and M. H M Abd El-Azim, "Green synthesis of zinc oxide nanoparticles using aqueous extract of deverra tortuosa and their cytotoxic activities," *Scientific Reports*, vol. 10, no. 1, p. 3445, 2020.

[64] J. Suresh, G. Pradheesh, V. Alexramani, M. Sundrarajan, and S. I. Hong, "Green synthesis and characterization of zinc oxide nanoparticle using insulin plant (*Costus pictus D. Don*) and investigation of its antimicrobial as well as anticancer activities," *Advances in Natural Sciences: Nanoscience and Nanotechnology*, vol. 9, no. 1, Article ID 015008, 2018.

[65] S. Imitan, S. Albonetti, L. Forni, F. Peri, and D. Lazzari, *Journal of Colloid and Interface Science*, vol. 329, p. 73, 2009.

[66] P. Sakthivel and S. Muthukumaram, *Journal of Physics and Chemistry of Solids*, vol. 120, p. 183, 2018.

[67] N. L. Tarwal, P. R. Jadhav, S. A. Vanalakar et al., "Photoluminescence of zinc oxide nanopowder synthesized by a combustion method," *Powder Technology*, vol. 208, no. 1, pp. 185–188, 2011.

[68] N. Talebian, M. Doudi, and H. Mogoei, "Antibacterial activities of sol–gel derived ZnO-multilayered thin films: p-NiO heterojunction layer effect," *Journal of Sol-Gel Science and Technology*, vol. 74, no. 3, pp. 650–660, 2015.

[69] M. Stan, A. Popa, D. Toloman, T. D. Silipas, and D. C. Vodnar, "Antibacterial and antioxidant activities of ZnO nanoparticles synthesized using extracts of Allium sativum, Rosmarinus officinalis and Ocimum basilicum," *Acta Metallurgica Sinica*, vol. 29, no. 3, pp. 228–236, 2016.

[70] A. Sirelkhatim, S. Mahmud, A. Seeni et al., "Review on zinc oxide nanoparticles: antibacterial activity and toxicity mechanism," *Nano-Micro Letters*, vol. 7, no. 3, pp. 219–242, 2015.

[71] H. Zulfiqar, A. Zafar, M. N. Rasheed et al., "Synthesis of silver nanoparticles using *Fagonia cretica* and their antimicrobial activities," *Nanoscale Advances*, vol. 1, no. 5, pp. 1707–1713, 2019.

[72] T. Thi, T. T. Nguyen, Y. D. Thi, K. H. T. Thi, B. T. Phan, and K. N. Pham, *RSC Advances*, vol. 10, Article ID 23899, 2020.

[73] M. I. Benitez- Salazar, V. E. Nino-Castano, R. A. Duenas-Cuellar, L. Caldas-Arias, I. Fernandez, and J. E. Rodríguez-Paez, *Journal of Environmental Chemical Engineering*, vol. 9, Article ID 106544, 2021.

[74] A. H. Moharram, S. A. Mansour, M. A. Hussein, and M. Rashad, "Direct precipitation and characterization of ZnO nanoparticles," *Journal of Nanomaterials*, vol. 2014, pp. 1–5, 2014.

[75] Z. N. Kayani, F. Saleemi, and I. Batool, "Effect of calcination temperature on the properties of ZnO nanoparticles," *Applied Physics*, vol. 119, no. 2, pp. 713–720, 2015.

[76] M. N. Siddique, T. Ali, A. Ahmed, and P. Tripathi, "Enhanced electrical and thermal properties of pure and Ni substituted ZnO Nanoparticles," *Nano-Structures & Nano-Objects*, vol. 16, pp. 156–166, 2018.